学位論文

Correlation Between Cardiac Images, Biomarkers, and Amyloid Load
in Wild-Type Transthyretin Amyloid Cardiomyopathy
（野生型トランスサイレチン型心アミロイドーシスにおける心筋イメージングとバイオマーカー、
病理学的なアミロイド沈着度の相関について）

森岡　真美

Mami　Morioka

熊本大学大学院医学教育部博士課程医学専攻循環器内科学

指導教員

辻田　賢一　教授

熊本大学大学院医学教育部博士課程医学専攻循環器内科学

2023 年 3 月

学 位 論 文

論文題名 ： Correlation Between Cardiac Images, Biomarkers, and Amyloid Load
in Wild-Type Transthyretin Amyloid Cardiomyopathy
（野生型トランスサイレチン型心アミロイドーシスにおける心筋イメージングとバイオマーカー、
病理学的なアミロイド沈着度の相関について）

著 者 名 ： 森岡 真美
Mami Morioka

指導教員名 ： 熊本大学大学院医学教育部博士課程医学専攻循環器内科学 辻田 賢一 教授

審査委員名 ： 心臓血管外科学担当教授 福井 寿啓 教授

細胞病理学担当教授 菰原 義弘 教授

臨床病態学担当教授 松井 啓隆 教授

脳神経内科学担当教授 三隅 洋平 講師

2023年3月

Journal of the American Heart Association

ORIGINAL RESEARCH

Correlation Between Cardiac Images, Biomarkers, and Amyloid Load in Wild-Type Transthyretin Amyloid Cardiomyopathy

Mami Morioka, MD; Seiji Takashio (iD), MD, PhD; Naoya Nakashima (iD), MD; Masato Nishi, MD; Akira Fujiyama, MD; Kyoko Hirakawa, MD, PhD; Shinsuke Hanatani (iD), MD, PhD; Hiroki Usuku (iD), MD, PhD; Eiichiro Yamamoto, MD, PhD; Masafumi Kidoh (iD), MD, PhD; Seitaro Oda (iD), MD, PhD; Kenichi Matsushita (iD), MD, PhD; Mitsuharu Ueda, MD, PhD; Kenichi Tsujita, MD, PhD

BACKGROUND: Several imaging parameters and biomarkers provide diagnostic and prognostic information for wild-type transthyretin amyloid cardiomyopathy. However, the relevance of these parameters and their association with cardiac amyloid load requires further substantiation. We aimed to elucidate the association of imaging parameters obtained using ^{99m}Tc-labeled pyrophosphate scintigraphy, cardiovascular magnetic resonance imaging, global longitudinal strain (GLS), and cardiac biomarkers with cardiac amyloid load in patients with wild-type transthyretin amyloid cardiomyopathy.

METHODS AND RESULTS: Eighty-eight patients with wild-type transthyretin amyloid cardiomyopathy who underwent ^{99m}Tc-labeled pyrophosphate scintigraphy and cardiovascular magnetic resonance were retrospectively evaluated. Quantitative cardiac amyloid load was obtained from 61 patients after myocardial biopsy. Correlations were assessed using Pearson's correlation coefficient applied to medical record data. The mean heart to contralateral ratio, native T1, extracellular volume, and GLS were 1.91±0.36, 1419.4±56.4 ms, 56.5±13.6%, and −9.4±2.5%, respectively. Median high-sensitivity cardiac troponin T (hs-cTnT) and BNP (B-type natriuretic peptide) levels were 0.0478 (0.0334-0.0691) ng/mL and 213.8 (125.8–392.7) pg/mL, respectively. The mean cardiac amyloid load was 22.9±15.0%. The heart to contralateral ratio correlated significantly with native T1 (r=0.397), extracellular volume (r=0.477), GLS (r=0.363), cardiac amyloid load (r=0.379), and Ln (hs-cTnT) (r=0.247). Further, cardiac amyloid load correlated significantly with native T1 (r=0.509), extracellular volume (r=0.310), GLS (r=0.446), and Ln (hs-cTnT) (r=0.354). Compared with BNP, hs-cTnT levels better correlated with several imaging parameters and cardiac amyloid load.

CONCLUSIONS: Increased cardiac amyloid load correlated with increased ^{99m}Tc-labeled pyrophosphate positivity, native T1, extracellular volume, and hs-cTnT levels, and an impaired GLS, suggesting that imaging parameters and cardiac biomarkers may reflect histological and functional changes attributable to amyloid deposition in the myocardium.

Key Words: amyloidosis ■ biomarkers ■ magnetic resonance imaging ■ ^{99m}Tc-labeled pyrophosphate pyrophosphate ■ troponin T

Transthyretin amyloid cardiomyopathy (ATTR-CM) is a progressive and infiltrative disease characterized by increased ventricular wall thickness, diastolic dysfunction, and cardiac conduction system alterations caused by the deposition of insoluble transthyretin amyloid fibrils in the extracellular space of the myocardium.[1] Although wild-type ATTR-CM (ATTRwt-CM) was previously considered a rare disease, recent diagnostic imaging modalities have revealed it to be considerably underdiagnosed among elderly patients with heart failure.[2,3] In addition, ATTRwt-CM has received considerable attention because of the development of novel disease-modifying treatments like tafamidis and patisiran.[4,5]

CLINICAL PERSPECTIVE

What Is New?

- The heart to contralateral ratio, native T1, extracellular volume, global longitudinal strain, and high-sensitivity cardiac troponin T levels correlate well with each other and with cardiac amyloid load in patients with wild-type transthyretin amyloid cardiomyopathy.
- While high-sensitivity cardiac troponin T levels correlated well with the heart-to-contralateral ratio, native T1, extracellular volume, global longitudinal strain, and cardiac amyloid load, B-type natriuretic peptide levels correlated only with extracellular volume and global longitudinal strain.

What Are the Clinical Implications?

- These imaging parameters and cardiac biomarkers are diagnostically and prognostically valuable in evaluating disease progression in patients with wild-type transthyretin amyloid cardiomyopathy.
- Their correlations may be used to predict cardiac amyloid load and determine the indications and therapeutic effects of disease-modifying therapies.

Nonstandard Abbreviations and Acronyms

99mTc-PYP	99mTc-labeled pyrophosphate
ATTR-CM	transthyretin amyloid cardiomyopathy
ATTRwt-CM	wild-type transthyretin amyloid cardiomyopathy
CPA	cardiac pyrophosphate activity
ECV	extracellular volume
GLS	global longitudinal strain
H/CL	heart to contralateral (ratio)

A systematic evaluation suggested that several imaging modalities and biomarkers are useful for the diagnostic and prognostic prediction of ATTR-CM. 99mTc-labeled pyrophosphate (99mTc-PYP) scintigraphy, or native T1 mapping and extracellular volume (ECV) measurements in cardiovascular magnetic resonance (CMR), are remarkably sensitive and specific for ATTR-CM diagnosis.[6–8] Moreover, marked 99mTc-PYP positivity and an elevated native T1 and ECV have been identified as predictors of poor prognosis in this condition.[7,9] Other parameters such as an impaired global longitudinal strain (GLS) on echocardiography[10] and elevated levels of high-sensitivity cardiac troponin T (hs-cTnT) and NT-proBNP (N-terminal pro-B-type natriuretic peptide),[11] are also associated with poor prognosis in patients with ATTRwt-CM. These reports suggest that 99mTc-PYP positivity as well as native T1, ECV, GLS, and cardiac biomarkers are related to disease progression in ATTR-CM.

Regarding histological findings, it has been reported that an extensive cardiac amyloid load is predictive of poor clinical outcomes and resistance to chemotherapy in light-chain amyloidosis.[12] We hypothesized that cardiovascular imaging findings, cardiac biomarkers, and pathological findings would reflect the progression of cardiac amyloidosis and that the cardiac amyloid load would have a close relationship with these parameters. If our hypothesis was true, these correlations might allow for noninvasive estimation of amyloid deposits, which to date can only be assessed by invasive means.

Thus, this study aimed to elucidate the associations among images obtained using several disease-specific modalities (99mTc-PYP scintigraphy, CMR, and echocardiography), cardiac biomarker levels (hs-cTnT and BNP [B-type natriuretic peptide]), and the histological cardiac amyloid load in patients with ATTRwt-CM.

METHODS

The data that support the findings of this study are available from the corresponding author upon reasonable request.

The study conformed to the principles outlined in the Declaration of Helsinki and was approved by the Institutional Review Board and Ethics Committee of Kumamoto University (Approval No. 1385). The requirement for informed consent was waived because of the low-risk nature of this retrospective study and the inability to obtain consent directly from all subjects. Instead, we extensively announced this study protocol at Kumamoto University Hospital and on our website (http://www.kumadai-junnai.com) and provided patients with the opportunity to withdraw from it.

Study Population

A total of 88 consecutive patients with ATTRwt-CM, who simultaneously underwent both 99mTc-PYP scintigraphy and CMR for evaluation of cardiac amyloidosis between March 2017 and October 2021 at Kumamoto University Hospital, were evaluated. Data were retrieved from electronic medical records. All study patients underwent echocardiography and laboratory testing in a clinically stable, noncongested condition at diagnosis.

Diagnosis of ATTR-CM and Genetic Testing

The diagnosis of amyloid deposition was based on the observation of apple-green birefringence in biopsies

stained with Congo red using cross-polarized light microscopy. To confirm the nature of the amyloid, we performed immunohistochemical staining using antibodies that reacted with transthyretin. ATTR-CM was diagnosed in the following cases: (1) presence of transthyretin deposition in the myocardium, (2) presence of transthyretin deposition in extracardiac tissue with positive findings on the ^{99m}Tc-PYP scintigraph, or (3) positive findings on the ^{99m}Tc-PYP scintigraph without confirmation of pathological transthyretin deposition but with the exclusion of light-chain amyloidosis by serum and urine protein electrophoresis and immunofixation. ATTRwt was diagnosed based on the absence of mutations in the *TTR* gene (assessed by genetic testing) or, in elderly patients, the absence of a family history of amyloidosis if genetic testing was not performed.

According to the diagnostic criteria of cardiac amyloidosis in the Japanese Circulation Society guideline,[13] the confirmation of histologically amyloid deposition in cardiac or extracardiac tissue is necessary to definitively diagnose ATTR-CM. In addition to the necessity of pathological diagnosis in patients with hematological abnormalities, we had to confirm the histological diagnosis to use tafamidis in Japan. Therefore, we performed an extracardiac biopsy, even though noninvasive diagnostic criteria were applied.

^{99m}Tc-PYP Scintigraphy Protocol

^{99m}Tc-PYP scintigraphy was performed using a GE Discovery 670 dual-headed single-photon emission computed tomography camera with low-energy, high-resolution collimators (GE Healthcare, Waukesha, WI). Anterior and lateral planar views of the heart were obtained 3 hours after radiotracer administration. ^{99m}Tc-PYP scintigraphy was assessed both planar and single-photon emission computed tomography images and scored by board-certified cardiovascular radiologists at our institution using the following grading system: grade 0, no cardiac uptake; grade 1, mild uptake, less than that of bone; grade 2, moderate uptake equal to that of bone; and grade 3, high uptake, greater than that of bone. ^{99m}Tc-PYP positivity was defined as a visual score of 2 or 3.[14] Quantitative analysis of cardiac retention was assessed using the heart to contralateral (H/CL) ratio of total counts in a region of interest over the heart to background counts in an identically sized region of interest over the contralateral chest, including soft tissue, ribs, and blood pool.[15] Furthermore, the direct radiotracer uptake in the myocardium was quantitatively evaluated using single-photon emission computed tomography images in patients with analyzable images, according to the protocol in a previous report.[16] First, a spherical region of interest was placed in the left ventricular blood pool to determine background radiotracer counts. Scan-specific thresholds for abnormal myocardial activity were determined as 1.5 × blood pool maximal radiotracer counts. Next, a polygonal region of interest was placed to encompass the left and right ventricular myocardium. Radiotracer activity in the myocardium was quantified as volume of abnormal activity and termed *volume of involvement*. Cardiac pyrophosphate activity (CPA), which reflects the volume and intensity of abnormal activity, was calculated as follows: CPA=volume of involvement×mean radiotracer counts of regions with abnormal myocardial activity/maximal blood pool radiotracer activity.

CMR Protocol

CMR was performed using a 3.0T MR scanner (Ingenia CX; Philips Healthcare, Best, The Netherlands) with a 16-channel coil. Pre- and postcontrast (15 minutes) T1 mapping was performed in a single midventricular short-axis slice (section thickness, 8 mm) using the shortened modified Look-Locker inversion recovery sequence (normal values, 1200–1260 ms in our institute). A gadolinium-based contrast material (0.2 mmol/kg, Gadovist; Bayer Yakuhin, Ltd., Osaka, Japan) was used.

The T1 mapping-derived myocardial ECV was calculated using the following formula: ECV (%)=(1−hematocrit) × (ΔR1 in myocardium) / (ΔR1 in the left ventricle) × 100. The calculated ECV values for the septal segment were assessed, which is recommended as a reproducible standard evaluation method for diffuse heart disease.[17] The 2 reviewers (M.K. and S.O.) were always blinded to the patient's clinical history and data to minimize bias.

Biomarker and Imaging Analysis

Serum hs-cTnT levels (normal cutoff value 0.014 pg/mL) were measured at diagnosis using the Elecsys 2010 Troponin T hs kit (Roche Diagnostics, Indianapolis, IN). Plasma BNP levels (normal cutoff value 18.4 pg/mL) were measured using the MI02 Shionogi BNP kit (Abbott Japan, Matsudo, Japan). The glomerular filtration rate was calculated using the Modification of Diet in Renal Disease Study equation, level-modified for Japanese people.

Echocardiographic Analysis

Echocardiography was performed using commercially available ultrasound equipment, including a Vivid E95 or 7 (GE Vingmed, Horten, Norway), Aplio 500 (Toshiba, Tokyo, Japan), or Epiq 7G (Philips, Bothell, WA). Cardiac chamber size and wall thickness were measured in the transthoracic view. The left ventricular ejection fraction (LVEF) was calculated using the modified Simpson's method. Two-dimensional strain analysis was performed using a vendor-independent software program (2D Strain Analysis; TOMTEC Imaging Systems,

Unterschleissheim, Germany). The left ventricular (LV) GLS was calculated as the average longitudinal strain of 16 segments of the LV, in accordance with the American Society for Echocardiography guideline.[18]

Quantitative Evaluation of Cardiac Amyloid Load

The cardiac amyloid load in myocardium biopsy specimens obtained from the right ventricular septum was quantitatively evaluated using ImageJ version 1.52a (National Institutes of Health, Bethesda, MD). The amyloid deposition area (observed by Congo red staining) and the total myocardium area were evaluated by adjusting the color threshold. The cardiac amyloid load was calculated as follows: cardiac amyloid load (%)=(amyloid deposition area / total myocardium area)×100 (Figure 1). The reviewers (M.M. and S.T.) were always blinded to the patients' clinical data.

Statistical Analysis

Normally distributed parameters are reported as mean±SD, while variables with skewed distributions are expressed as medians (interquartile range). Categorical values are presented as numbers and percentages. Correlations between parameters were assessed using Pearson's correlation coefficient. BNP and hs-cTnT levels were logarithmically transformed before calculating the Pearson's correlation because they were not normally distributed. Multiple linear regression analyses were used to identify variables that might predict cardiac amyloid load, including H/CL ratio, native T1, ECV, GLS, BNP, and hs-cTnT levels. All statistical analyses were performed using the Statistical Package for Social Sciences, version 19 (SPSS Inc., Chicago, IL).

RESULTS
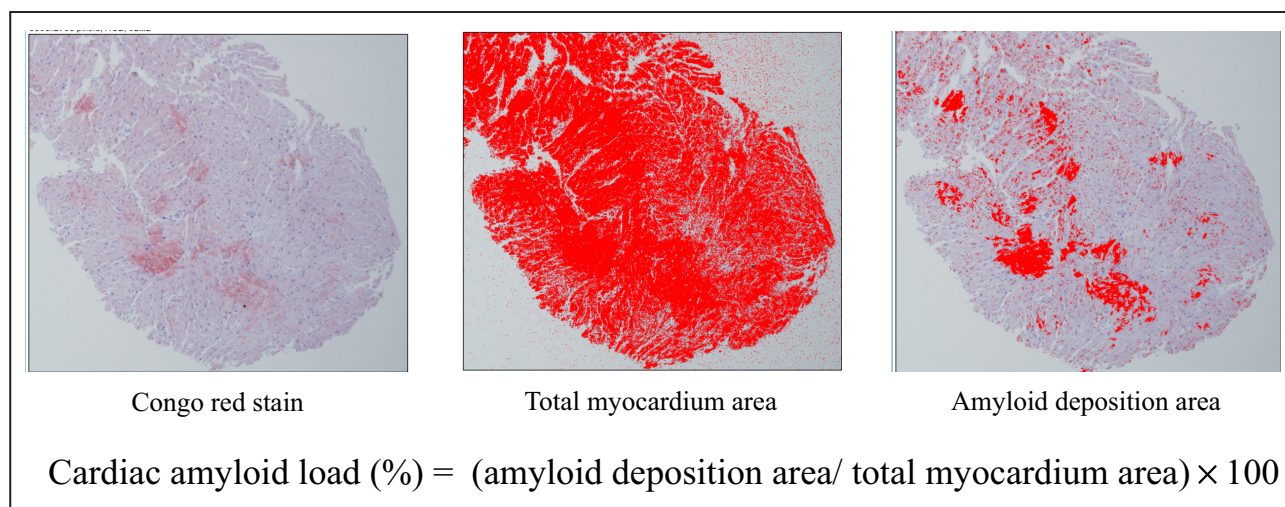
Clinical Characteristics

Demographic characteristics of the study population are presented in Table 1. Patients were predominantly male (90%) and elderly (75.4±6.1 years). Median hs-cTnT and BNP levels were elevated. Echocardiographic findings were characterized by a LVEF and symmetrical LV wall thickening, which was attributed to infiltrative amyloid deposition. Despite a preserved LVEF, the GLS was considerably depressed (–9.4±2.5%).

Overall, 69 patients (78%) showed myocardial transthyretin deposition. Of the remaining patients, 16 had extracardiac transthyretin deposition with positive ^{99m}Tc-PYP scintigraphy, and 3 had positive ^{99m}Tc-PYP scintigraphy and absence of detectable monoclonal protein. Genetic testing was performed in 82 patients (93%) and was negative for *TTR* mutation in all cases; the remaining 6 patients were octogenarians and had no family history of amyloidosis. Therefore, all patients were diagnosed with ATTRwt-CM.

By ^{99m}Tc-PYP scintigraphy, the mean H/CL ratio was 1.91±0.36 and CPA was 233.8±180.8 cm^3 (n=69). Regarding CMR imaging, 4 patients could not be evaluated for ECV because of contraindications of contrast media caused by renal failure. Cardiac amyloid load was calculated in 61 of 69 patients who had amyloid deposition in the myocardium; the mean cardiac amyloid load was 22.9±15.0%.

Comparison of Clinical Characteristics Between the High and Low Cardiac Amyloid Load Groups

Differences in the demographic and clinical characteristics between the 2 groups divided by median amyloid

Congo red stain   Total myocardium area   Amyloid deposition area

$$\text{Cardiac amyloid load (\%)} = (\text{amyloid deposition area} / \text{total myocardium area}) \times 100$$

Figure 1. Calculation of cardiac amyloid load.
The cardiac amyloid load in myocardium biopsy specimens was evaluated using ImageJ. The amyloid deposition area was stained with Congo red, and the total myocardium area was evaluated by adjusting the color threshold.

Table 1. Demographic and clinical characteristics of participants (n=88)

Variable	
Age, y	75.4±6.1
Male sex	79 (90)
NYHA functional class (I/II/III/IV)	19/41/27/1
Prior heart failure hospitalization, n (%)	24 (27)
Blood testing	
Sodium, mmol/L	140.1±2.5
Creatinine, mg/dL	1.03±0.27
eGFR, mL/min per 1.73 m^2	55.8±13.3
Hemoglobin, g/dL	13.7±1.8
hs-cTnT, ng/mL	0.048 (0.033–0.069)
BNP, pg/mL)	213.8 (125.8–392.7)
Medications	
Loop diuretics	53 (60)
Beta blockers	20 (23)
RAS inhibitors	33 (38)
Aldosterone antagonists	23 (26)
Echocardiogram parameter	
LVDd, mm	42.2±5.7
LVDs, mm	31.9±6.3
IVSd, mm	15.1±2.3
LVPWd, mm	15.5±2.8
LAD, mm	42.9±8.5
LVEF, %	51.9±10.6
E/e′	20.1±7.8
GLS, %	-9.4±2.5
^{99m}Tc-PYP scintigraphy parameters	
H/CL ratio	1.91±0.36
CPA, cm^{3*}	233.8±180.8
CMR parameters	
ECV, %[†]	56.5±13.6
Native T1 value, ms	1419.4±56.4
LVMI, g/m^2	83.0±29.4
LVEF, %	51.5±14.8
Histological parameters	
Amyloid load, %[‡]	22.9±15.0

Data are presented as median (interquartile range), mean±standard deviation, or n (%). BNP indicates B-type natriuretic peptide; CMR, cardiovascular magnetic resonance imaging; CPA, cardiac pyrophosphate activity; ECV, extracellular volume; eGFR, estimated glomerular filtration rate; GLS, global longitudinal strain; H/CL, heart to contralateral; hs-cTnT, high-sensitivity cardiac troponin T; LAD, left atrial diameter; IVSd, interventricular septum diameter; LVDd, left ventricular diastolic diameter; LVDs, left ventricular systolic diameter; LVEF, left ventricular ejection fraction; LVMI, left ventricular mass index; LVPWd, left ventricular posterior wall diameter; NYHA, New York Heart Association; RAS, renin-angiotensin system; and ^{99m}Tc-PYP, ^{99m}Tc-labeled pyrophosphate.

*n=69.

[†]n=84.

[‡]n=61.

load (21.2%) are presented in Table 2. In the high cardiac amyloid load group, the patients were comparatively younger (72.7±5.5 years versus 76.3±5.7 years;

P=0.014), and the proportion of men was higher (97% versus 77%; P=0.020). The hs-cTnT and hemoglobin levels, H/CL ratios, CPA, native T1, and LV mass indices were significantly higher in the high cardiac amyloid load group. GLS and LVEF measured by CMR were impaired in the high cardiac amyloid load group when compared with those of the low cardiac amyloid load group.

Correlation Between Image Parameters, Histology Findings, and Biomarkers

All correlation data are shown in Table 3. The H/CL ratio, native T1, ECV, GLS, hs-cTnT, and cardiac amyloid load were significantly correlated with each other (P<0.05). The H/CL ratio was significantly and positively correlated with native T1 (r=0.397, P=0.001), ECV (r=0.477, P<0.001), GLS (r=0.363, P=0.001), cardiac amyloid load (r=0.379, P=0.003), and Ln(hs-cTnT) levels (r=0.247, P=0.020; Figure 2). Cardiac amyloid load was also significantly and positively correlated with native T1 (r=0.509, P<0.001), ECV (r=0.310, P=0.018), GLS (r=0.446, P<0.001), and Ln(hs-cTnT) (r=0.354, P=0.005; Figure 3).

On the other hand, BNP levels had limited correlation with native T1 (r=0.249, P=0.021), ECV (r=0.284, P=0.01), and GLS (r=0.280, P=0.009). The hs-cTnT levels correlated significantly with more assessment parameters than reported for BNP (H/CL ratio, r=0.247, P=0.02; native T1, r=0.409, P<0.001; ECV, r=0.410, P<0.001; GLS, r=0.503, P<0.001; and cardiac amyloid load, r=0.354, P=0.005). The CPA, LV mass index and LVEF obtained by CMR had significant correlation with several assessment parameters (Table 3).

In multiple linear regression analyses including H/CL ratio, native T1, ECV, GLS, BNP, and hs-cTnT levels, native T1 (standardized regression coefficient, 0.374; P=0.008) and GLS (standardized regression coefficient, 0.366; P=0.009) were independent predictor of cardiac amyloid load.

DISCUSSION

In this study, we found a significant correlation between imaging, histological, and serological parameters that have diagnostic and prognostic value in patients with ATTRwt-CM. The major findings are as follows: (1) the H/CL ratio, native T1, ECV, LV mass index, LVEF, GLS, hs-cTnT level, and cardiac amyloid load are significantly correlated with each other; (2) an elevated H/CL ratio, native T1, ECV, LV mass index, LVEF and hs-cTnT level, and an impaired GLS are all related to an increased cardiac amyloid load; and (3) hs-cTnT levels showed a better correlation with several parameters when compared the correlation to BNP levels. To the best of our knowledge, this is the first study to evaluate the association of several

Table 2. Differences in demographic and clinical characteristics between the high and low cardiac amyloid load groups

Variables	High amyloid load group (n=31)	Low amyloid load group (n=30)	P value
Age, y	72.7±5.5	76.3±5.7	0.014
Male sex	30 (97)	23 (77)	0.020
Prior heart failure hospitalization	10 (32%)	10 (33%)	0.930
Blood testing			
Sodium, mmol/L	139.7±2.4	140.5±2.2	0.181
Creatinine, mg/dL	1.03±0.24	0.97±0.17	0.242
eGFR, mL/min per 1.73 m^2	55.9±11.9	56.3±12.2	0.907
Hemoglobin, g/dL	14.3±1.9	13.3±1.7	0.031
hs-cTnT, ng/mL	0.048 (0.034–0.086)	0.042 (0.030–0.064)	0.037
BNP, pg/mL	213.8 (113.8–424.1)	205.3 (128.5–372.2)	0.878
Echocardiogram parameters			
LVDd, mm	43.1±6.0	41.2±5.4	0.198
LVDs, mm	33.1±6.4	30.7±6.1	0.137
IVSd, mm	15.4±2.0	15.0±2.6	0.442
LVPWd, mm	16.1±2.3	15.3±2.8	0.267
LVEF, %	49.8±11.2	53.3±10.0	0.204
GLS, %	−8.3±2.0	−10.1±2.2	0.002
99mTc-PYP scintigraphy parameters			
H/CL ratio	2.04±0.36	1.82±0.31	0.014
CPA, cm^3	330.0±234.2 (n=23)	187.9±127.6 (n=22)	0.015
CMR parameters			
ECV, %	60.2±12.6	55.1±12.6	0.135
Native T1 value, ms	1449.9±42.8	1400.2±53.0	<0.001
LV mass index, g/m^2	92.9±32.1	74.4±23.2	0.016
LVEF, %	46.7±12.5	55.8±13.3	0.008

Data are presented as median (interquartile range), mean±standard deviation, or n (%). BNP indicates B-type natriuretic peptide; CMR, cardiovascular magnetic resonance imaging; CPA, cardiac pyrophosphate activity; ECV, extracellular volume; eGFR, estimated glomerular filtration rate; GLS, global longitudinal strain; H/CL, heart to contralateral; hs-cTnT, high-sensitivity cardiac troponin T; IVSd, interventricular septum diameter; LVDd, left ventricular diastolic diameter; LVDs, left ventricular systolic diameter; LVEF, left ventricular ejection fraction; LVMI, left ventricular mass index; LVPWd, left ventricular posterior wall diameter; and 99mTc-PYP, 99mTc-labeled pyrophosphate.

diagnostic and prognostic parameters evaluated by different imaging modalities, cardiac biomarker levels, and historical findings in patients with ATTRwt-CM.

What does the accumulation of 99mTc-PYP and the increase of native T1 and ECV reflect in ATTR-CM? Although the mechanism of myocardial 99mTc-PYP uptake in ATTR-CM is not fully understood, the binding of the radiotracer to microcalcifications may explain the increased uptake compared with light-chain amyloidosis.[19] Since the ECV is based on the signal from the extracellular space, and native T1 is related to both intracellular and extracellular edema, they are potentially subject to the influence of other pathophysiological mechanisms beyond amyloid load.[20,21] Therefore, it is considered that native T1 and ECV not only reflect amyloid deposition in the myocardium but also reflect reactive changes like fibrosis and edema. Based on these assumptions, these modalities are considered to correlate with each other, although few reports have addressed this issue specifically until now.

In this study, we confirmed the assumption of correlation. In this regard, Martinez-Naharro et al[7] had reported that, in patients with ATTR-CM, native T1 and ECV had good correlation with each other (r=0.726) and were associated with the grade of cardiac uptake in bone scintigraphy. However, no analyses regarding quantitative 99mTc-PYP positivity and CMR findings were conducted in their study. Considering the results of our study, native T1, ECV, and H/CL ratio may similarly reflect the pathological status and progression of ATTR-CM.

The mean cardiac amyloid load in this study was 22.9%. Analyzing 74 patients with ATTRwt-CM, Kristen et al[12] reported a comparatively higher mean cardiac amyloid load (34.0%). However, subjects in their study had a thicker septal wall (median, 20 mm) and lower LVEF (median, 42.7%) than our subjects, which is characteristic of more advanced disease. We classified the high and low amyloid load groups by median value (21.2%). The high amyloid load group was younger

Table 3. Correlations between imaging modalities, cardiac amyloid load, and serum biomarkers

	H/CL ratio	CPA	Native T1	ECV	LVMI	GLS	Amyloid load	Ln (BNP)	Ln (hsTnT)	LVEF (CMR)
H/CL ratio		0.265*	0.397†	0.477†	0.269*	0.363†	0.379†	−0.116	0.247*	−0.243*
CPA	0.265*		0.296*	0.316†	0.463†	0.216	0.413†	0.164	0.145	−0.167
Native T1	0.397†	0.296*		0.549†	0.414†	0.425†	0.509†	0.249*	0.409†	−0.476†
ECV	0.477†	0.316†	0.549†		0.516†	0.519†	0.310*	0.284†	0.410†	−0.524†
LVMI	0.269*	0.463†	0.414†	0.516†		0.420†	0.529†	0.422†	0.535†	−0.347†
GLS	0.363†	0.216	0.425†	0.519†	0.420†		0.446†	0.280†	0.503†	−0.580†
Amyloid load	0.379†	0.413†	0.509†	0.310*	0.529†	0.446*		0.069	0.354†	−0.331†
Ln (BNP)	−0.166	0.164	0.249*	0.284†	0.422†	0.280†	0.069		0.448†	−0.155
Ln (hsTnT)	0.247*	0.145	0.409†	0.410†	0.535†	0.503†	0.354†	0.448†		−0.408†
LVEF (CMR)	−0.243*	−0.167	−0.476†	−0.524†	−0.347†	−0.580†	−0.331†	−0.155	−0.448†	

Values correspond to correlation coefficient (r). BNP indicates B-type natriuretic peptide; CMR, cardiovascular magnetic resonance; CPA, cardiac pyrophosphate activity; ECV, extracellular volume; GLS, global longitudinal strain; H/CL, heart to contralateral; hs-cTnT, high-sensitivity cardiac troponin T; LVEF, left ventricular ejection fraction; and LVMI, left ventricular mass index.

*$P<0.05$.
†$P<0.01$.

than the low amyloid load group (72.7±5.5 years versus 76.3±5.7 years). This result was inconsistent that ATTRwt-CM is a progressive disease associated with aging. We had to confirm the histological diagnosis to use tafamidis in Japan. Therefore, myocardial biopsy was performed in younger patients considering tafamidis administration and might be avoided in elderly advanced patients. This selection bias may cause this discrepancy.

In our study, native T1 had a better correlation with cardiac amyloid load than ECV. While native T1 is a myocardial parameter obtained directly without the need for contrast enhancement, ECV is calculated using multiple variables (pre- and postcontrast myocardial and blood T1 values and hematocrit). Considering that gadolinium washout may be influenced by extracardiac factors like the total body amyloid load and impaired renal function,[22] this may be a reason for the weaker correlation observed between ECV and cardiac amyloid load when compared with the correlation with native T1. Recently, several studies reported that disease-specific treatment for ATTR-CM can delay the structural and functional progression evaluated by CMR. Considering these results together with our results, disease-specific treatment may suppress the progression of amyloid deposition in the myocardium.[23–26]

In cardiac amyloidosis, GLS has shown to be a reliable measurement of systolic function and an independent predictor of mortality.[10] In our study, GLS significantly correlated with ^{99m}Tc-PYP positivity, native T1, ECV, cardiac amyloid load, and cardiac biomarker levels. Treatment with patisiran, an RNA interference therapeutic agent that inhibits transthyretin synthesis for up to 18 months, results in GLS improvement in patients with hereditary ATTR-CM.[27] If GLS correlates with the progression of pathological and functional conditions, it may be useful for monitoring ATTR-CM disease progression and assessing the therapeutic effect of disease-specific agents.

In previous reports, increased hs-cTnT and NT-proBNP levels were associated with a poor outcome in patients with ATTRwt-CM, when used separately or in combination.[11] Therefore, we hypothesized that these laboratory parameters would correlate with imaging and pathological findings. While hs-cTnT correlated well with the H/CL ratio, native T1, ECV, GLS, and cardiac amyloid load, BNP did so only with ECV and GLS. This is not surprising because these 2 molecules relate to different pathophysiological aspects. While cardiac troponin T is a specific and sensitive marker of myocardial injury,[28] BNP is considered a sensitive indicator of cardiac overload.[29] Persistent hypertroponinemia is considered a red flag for cardiac amyloidosis.[30,31] The exact mechanism responsible for
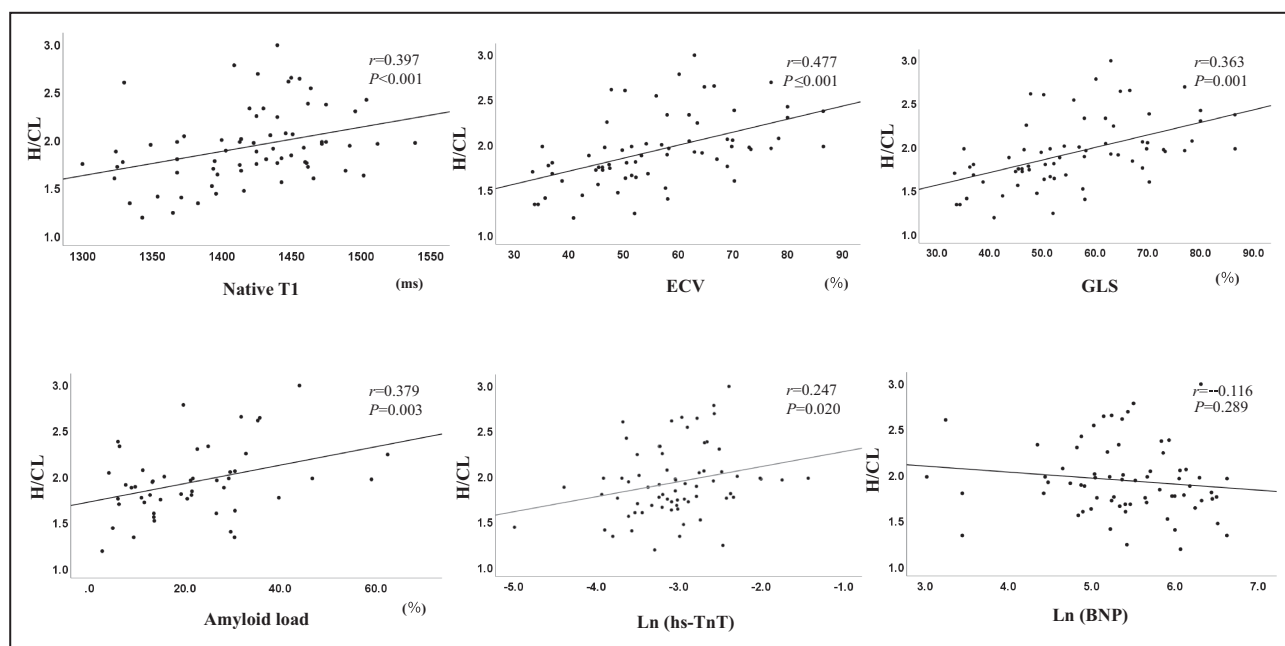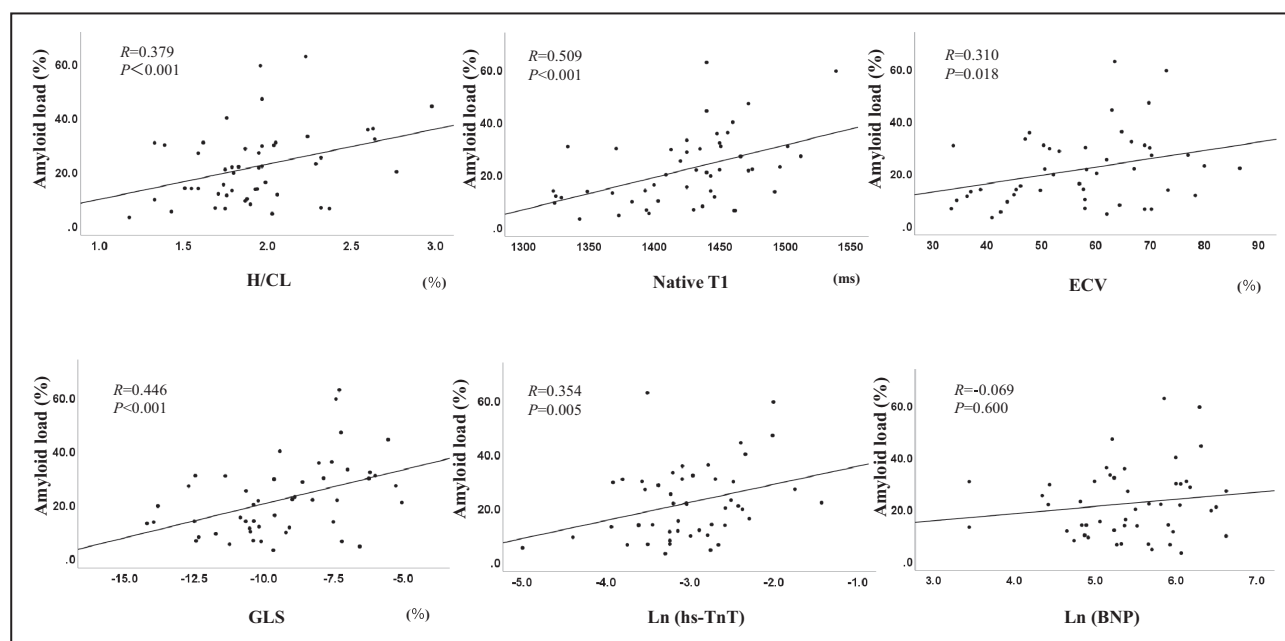
Figure 2. Correlation between the H/CL ratio and other assessment parameters.
The H/CL ratio was positively correlated with native T1, ECV, GLS, cardiac amyloid load, and hs-cTnT levels. BNP indicates B-type natriuretic peptide; ECV, extracellular volume; GLS, global longitudinal strain; H/CL, heart to contralateral; and hs-cTnT, high-sensitivity cardiac troponin T.

persistent hypertroponinemia in patients with cardiac amyloidosis remains speculative, but potential mechanisms include myocardial damage due to coronary microvascular dysfunction[32] or increased diastolic load.[33] These impairments are thought to be associated with increased amyloid load. Considering the above, cardiac troponin seems to be more reflective of the progression of amyloid cardiomyopathy than BNP.

Figure 3. Correlation between cardiac amyloid load and other assessment parameters.
Cardiac amyloid load was positively correlated with H/CL ratio, native T1, ECV, GLS, and hs-cTnT levels. BNP indicates B-type natriuretic peptide; ECV, extracellular volume; GLS, global longitudinal strain; H/CL, heart to contralateral ratio; and hs-cTnT, high-sensitivity cardiac troponin T.

Limitations

This study had several limitations. First, it had a small sample size and was conducted at a single center. Second, endomyocardial biopsy may not accurately reflect the total myocardial amyloid load in patients with ATTR-CM because transthyretin deposition has been reported to be patchy and of varied individual size.[12,34] Therefore, the amount of amyloid deposition may depend on the biopsy site. Third, hs-cTnT levels are affected by impaired renal function and myocardial ischemia. Bias in this regard was minimized by measuring hs-cTnT levels in clinically stable patients and excluding concomitant coronary stenosis in 65 patients using coronary angiography. Fourth, 6 patients lacked a confirmed pathological diagnosis of transthyretin. However, CMR and ^{99m}Tc-PYP findings in these patients were consistent with amyloidosis, monoclonal gammopathy assessments were negative, and clinical diagnostic criteria for ATTR-CM were met.[6] Fifth, we evaluated the patients' clinical performance only with New York Heart Association functional class, not the 6-minute walk time and the Kansas City Cardiomyopathy Questionnaire. In addition, we did not provide serial measurement and clinical outcome data related to imaging and pathological findings. Finally, the H/CL ratio is influenced by regional rib radiotracer uptake and radiotracer retention in the LV blood pool. To compensate for this limitation, we performed quantitative evaluation of radiotracer uptake in the myocardium via single-photon emission computed tomography and clarified the correlation between CPA and amyloid deposition. However, this analysis was performed on a limited number of patients and needs further verification.

CONCLUSIONS

In this study, we confirmed our hypothesis that ^{99m}Tc-PYP positivity (H/CL ratio), CMR parameters (native T1 and ECV), GLS, and hs-cTnT levels have a good correlation with each other. This result is important regarding the monitoring of ATTRwt-CM progression. In addition, these parameters are associated with cardiac amyloid load, suggesting that they reflect the degree of transthyretin amyloid deposition in the myocardium. Further studies with larger sample sizes are needed to validate our results and evaluate the utility of each modality, not only as diagnostic and prognostic tools but also as indicators of clinical efficacy and regression of amyloid deposition during the administration of novel disease-modifying treatments.

ARTICLE INFORMATION

Affiliations

Departments of Cardiovascular Medicine (M.M., S.T., N.N., M.N., A.F., K.H., S.H., H.U., E.Y., K.M., K.T.), Departments of Diagnostic Radiology (M.K., S.O.) and Departments of Neurology (M.U.), Graduate School of Medical Sciences, Kumamoto University, Kumamoto, Japan.

Acknowledgments

Sources of Funding

Disclosures

None.

REFERENCES

1. Ruberg FL, Berk JL. Transthyretin (TTR) cardiac amyloidosis. *Circulation*. 2012;126:1286–1300. doi: 10.1161/CIRCULATIONAHA.111.078915

2. Mohammed SF, Mirzoyev SA, Edwards WD, Dogan A, Grogan DR, Dunlay SM, Roger VL, Gertz MA, Dispenzieri A, Zeldenrust SR, et al. Left ventricular amyloid deposition in patients with heart failure and preserved ejection fraction. *JACC Heart Fail*. 2014;2:113–122. doi: 10.1016/j.jchf.2013.11.004

3. González-López E, Gallego-Delgado M, Guzzo-Merello G, de Haro-del Moral FJ, Cobo-Marcos M, Robles C, Bornstein B, Salas C, Lara-Pezzi E, Alonso-Pulpon L, et al. Wild-type transthyretin amyloidosis as a cause of heart failure with preserved ejection fraction. *Eur Heart J*. 2015;36:2585–2594. doi: 10.1093/eurheartj/ehv338

4. Maurer MS, Schwartz JH, Gundapaneni B, Elliott PM, Merlini G, Waddington-Cruz M, Kristen AV, Grogan M, Witteles R, Damy T, et al. Tafamidis treatment for patients with transthyretin amyloid cardiomyopathy. *N Engl J Med*. 2018;379:1007–1016. doi: 10.1056/NEJMoa1805689

5. Adams D, Gonzalez-Duarte A, O'Riordan WD, Yang C-C, Ueda M, Kristen AV, Tournev I, Schmidt HH, Coelho T, Berk JL, et al. Patisiran, an RNAi therapeutic, for hereditary transthyretin amyloidosis. *N Engl J Med*. 2018;379:11–21. doi: 10.1056/NEJMoa1716153

6. Gillmore JD, Maurer MS, Falk RH, Merlini G, Damy T, Dispenzieri A, Wechalekar AD, Berk JL, Quarta CC, Grogan M, et al. Nonbiopsy diagnosis of cardiac transthyretin amyloidosis. *Circulation*. 2016;133:2404–2412. doi: 10.1161/CIRCULATIONAHA.116.021612

7. Martinez-Naharro A, Kotecha T, Norrington K, Boldrini M, Rezk T, Quarta C, Treibel TA, Whelan CJ, Knight DS, Kellman P, et al. Native T1 and extracellular volume in transthyretin amyloidosis. *JACC Cardiovasc Imaging*. 2019;12:810–819. doi: 10.1016/j.jcmg.2018.02.006

8. Vogelsberg H, Mahrholdt H, Deluigi CC, Yilmaz A, Kispert EM, Greulich S, Klingel K, Kandolf R, Sechtem U. Cardiovascular magnetic resonance in clinically suspected cardiac amyloidosis: noninvasive imaging compared to endomyocardial biopsy. *J Am Coll Cardiol*. 2008;51:1022–1030. doi: 10.1016/j.jacc.2007.10.049

9. Castano A, Haq M, Narotsky DL, Goldsmith J, Weinberg RL, Morgenstern R, Pozniakoff T, Ruberg FL, Miller EJ, Berk JL, et al. Multicenter study of planar technetium 99m pyrophosphate cardiac imaging: predicting survival for patients with ATTR cardiac amyloidosis. *JAMA Cardiol*. 2016;1:880–889. doi: 10.1001/jamacardio.2016.2839

10. Chacko L, Martone R, Bandera F, Lane T, Martinez-Naharro A, Boldrini M, Rezk T, Whelan C, Quarta C, Rowczenio D, et al. Echocardiographic phenotype and prognosis in transthyretin cardiac amyloidosis. *Eur Heart J*. 2020;41:1439–1447. doi: 10.1093/eurheartj/ehz905

11. Grogan M, Scott CG, Kyle RA, Zeldenrust SR, Gertz MA, Lin G, Klarich KW, Miller WL, Maleszewski JJ, Dispenzieri A. Natural history of wild-type transthyretin cardiac amyloidosis and risk stratification using a novel staging system. *J Am Coll Cardiol*. 2016;68:1014–1020. doi: 10.1016/j.jacc.2016.06.033

12. Kristen AV, Brokbals E, aus dem Siepen F, Bauer R, Hein S, Aurich M, Riffel J, Behrens H-M, Krüger S, Schirmacher P, et al. Cardiac amyloid load: a prognostic and predictive biomarker in patients with light-chain amyloidosis. *J Am Coll Cardiol*. 2016;68:13–24. doi: 10.1016/j.jacc.2016.04.035

13. Kitaoka H, Izumi C, Izumiya Y, Inomata T, Ueda M, Kubo T, Koyama J, Sano M, Sekijima Y, Tahara N, et al. JCS 2020 guideline on diagnosis and treatment of cardiac amyloidosis. *Circ J*. 2020;84:1610–1671. doi: 10.1253/circj.CJ-20-0110

14. Dorbala S, Ando Y, Bokhari S, Dispenzieri A, Falk RH, Ferrari VA, Fontana M, Gheysens O, Gillmore JD, Glaudemans AWJM, et al. ASNC/AHA/ASE/EANM/HFSA/ISA/SCMR/SNMMI expert consensus recommendations for multimodality imaging in cardiac amyloidosis: part 1 of 2-evidence base and standardized methods of imaging. *Circ Cardiovasc Imaging*. 2021;14:e000029. doi: 10.1161/HCI.0000000000000029

15. Bokhari S, Castaño A, Pozniakoff T, Deslisle S, Latif F, Maurer MS. (99m) Tc-pyrophosphate scintigraphy for differentiating light-chain cardiac amyloidosis from the transthyretin-related familial and senile cardiac amyloidoses. *Circ Cardiovasc Imaging*. 2013;6:195–201. doi: 10.1161/CIRCIMAGING.112.000132

16. Miller RJH, Cadet S, Mah D, Pournazari P, Chan D, Fine NM, Berman DS, Slomka PJ. Diagnostic and prognostic value of Technetium-99m pyrophosphate uptake quantitation for transthyretin cardiac amyloidosis. *J Nucl Cardiol*. 2021;28:1835–1845. doi: 10.1007/s12350-021-02563-4

17. Engblom H, Kanski M, Kopic S, Nordlund D, Xanthis CG, Jablonowski R, Heiberg E, Aletras AH, Carlsson M, Arheden H. Importance of standardizing timing of hematocrit measurement when using cardiovascular magnetic resonance to calculate myocardial extracellular volume (ECV) based on pre- and post-contrast T1 mapping. *J Cardiovasc Magn Reson*. 2018;20:46. doi: 10.1186/s12968-018-0464-9

18. Lang RM, Badano LP, Mor-Avi V, Afilalo J, Armstrong A, Ernande L, Flachskampf F, Foster E, Goldsetin SR, Kuznetsova T, et al. Recommendations for cardiac chamber quantification by echocardiography in adults: an update from the american society of echocardiography and the european association of, cardiovascular imaging. *Eur Heart J Cardiovasc Imaging*. 2016;17:412. doi: 10.1093/ehjci/jew041

19. Stats MA, Stone JR. Varying levels of small microcalcifications and macrophages in ATTR and AL cardiac amyloidosis: implications for utilizing nuclear medicine studies to subtype amyloidosis. *Cardiovasc Pathol*. 2016;25:413–417. doi: 10.1016/j.carpath.2016.07.001

20. Messroghli DR, Moon JC, Ferreira VM, Grosse-Wortmann L, He T, Kellman P, Mascherbauer J, Nezafat R, Salerno M, Schelbert EB, et al. Clinical recommendations for cardiovascular magnetic resonance mapping of T1, T2, T2* and extracellular volume: A consensus statement by the Society for Cardiovascular Magnetic Resonance (SCMR) endorsed by the European Association for Cardiovascular Imaging (EACVI). *J Cardiovasc Magn Reson*. 2017;19:75. doi: 10.1186/s12968-017-0389-8

21. Fontana M, Banypersad SM, Treibel TA, Maestrini V, Sado DM, White SK, Pica S, Castelletti S, Piechnik SK, Robson MD, et al. Native T1 mapping in transthyretin amyloidosis. *JACC Cardiovasc Imaging*. 2014;7:157–165. doi: 10.1016/j.jcmg.2013.10.008

22. Maceira AM, Joshi J, Prasad SK, Moon JC, Perugini E, Harding I, Sheppard MN, Poole-Wilson PA, Hawkins PN, Pennell DJ. Cardiovascular magnetic resonance in cardiac amyloidosis. *Circulation*. 2005;111:186–193. doi: 10.1161/01.CIR.0000152819.97857.9D

23. Fontana M, Martinez-Naharro A, Chacko L, Rowczenio D, Gilbertson JA, Whelan CJ, Strehina S, Lane T, Moon J, Hutt DF, et al. Reduction in CMR derived extracellular volume with Patisiran indicates cardiac amyloid regression. *JACC Cardiovasc Imaging*. 2021;14:189–199. doi: 10.1016/j.jcmg.2020.07.043

24. Rettl R, Mann C, Duca F, Dachs TM, Binder C, Ligios LC, Schrutka L, Dalos D, Koschutnik M, Donà C, et al. Tafamidis treatment delays structural and functional changes of the left ventricle in patients with transthyretin amyloid cardiomyopathy. *European Heart Journal - Cardiovascular Imaging*. 2021;10.1093/ehjci/jeab226. doi: 10.1093/ehjci/jeab226

25. Higaki JN, Chakrabartty A, Galant NJ, Hadley KC, Hammerson B, Nijjar T, Torres R, Tapia JR, Salmans J, Barbour R, et al. Novel conformation-specific monoclonal antibodies against amyloidogenic forms of transthyretin. *Amyloid*. 2016;23:86–97. doi: 10.3109/13506129.2016.1148025

26. Müller ML, Butler J, Heidecker B. Emerging therapies in transthyretin amyloidosis - a new wave of hope after years of stagnancy? *Eur J Heart Fail*. 2020;22:39–53. doi: 10.1002/ejhf.1695

27. Minamisawa M, Claggett B, Adams D, Kristen AV, Merlini G, Slama MS, Dispenzieri A, Shah AM, Falk RH, Karsten V, et al. Association of Patisiran, an RNA interference therapeutic, with regional left ventricular myocardial strain in hereditary transthyretin amyloidosis: The APOLLO study. *JAMA Cardiol*. 2019;4:466–472. doi: 10.1001/jamacardio.2019.0849

28. Kociol RD, Pang PS, Gheorghiade M, Fonarow GC, O'Connor CM, Felker GM. Troponin elevation in heart failure prevalence, mechanisms, and clinical implications. *J Am Coll Cardiol*. 2010;56:1071–1078. doi: 10.1016/j.jacc.2010.06.016

29. Daniels LB, Maisel AS. Natriuretic peptides. *J Am Coll Cardiol*. 2007;50:2357–2368. doi: 10.1016/j.jacc.2007.09.021

30. Ruberg FL, Grogan M, Hanna M, Kelly JW, Maurer MS. Transthyretin amyloid cardiomyopathy: JACC state-of-the-art review. *J Am Coll Cardiol*. 2019;73:2872–2891. doi: 10.1016/j.jacc.2019.04.003

31. Witteles RM, Bokhari S, Damy T, Elliott PM, Falk RH, Fine NM, Gospodinova M, Obici L, Rapezzi C, Garcia-Pavia P. Screening for transthyretin amyloid cardiomyopathy in everyday practice. *JACC Heart Fail*. 2019;7:709–716. doi: 10.1016/j.jchf.2019.04.010

32. Ogawa H, Mizuno Y, Ohkawara S, Tsujita K, Ando Y, Yoshinaga M, Yasue H. Cardiac amyloidosis presenting as microvascular angina–a case report. *Angiology*. 2001;52:273–278. doi: 10.1177/000331970105200407

33. Takashio S, Yamamuro M, Izumiya Y, Sugiyama S, Kojima S, Yamamoto E, Tsujita K, Tanaka T, Tayama S, Kaikita K, et al. Coronary microvascular dysfunction and diastolic load correlate with cardiac troponin T release measured by a highly sensitive assay in patients with nonischemic heart failure. *J Am Coll Cardiol*. 2013;62:632–640. doi: 10.1016/j.jacc.2013.03.065

34. Bergström J, Gustavsson A, Hellman U, Sletten K, Murphy CL, Weiss DT, Solomon A, Olofsson B, Westermark P. Amyloid deposits in transthyretin-derived amyloidosis: cleaved transthyretin is associated with distinct amyloid morphology. *J Pathol*. 2005;206:224–232. doi: 10.1002/path.1759